Supplementary information for *Tipping the ENSO into a permanent El Niño can trigger state transitions in global terrestrial ecosystems*

Mateo Duque-Villegas[1], Juan F. Salazar[1], and Angela M. Rendón[1]

[1]GIGA, Escuela Ambiental, Facultad de Ingeniería, Universidad de Antioquia, Medellín, Colombia

Correspondence: Juan F. Salazar (juan.salazar@udea.edu.co)

List of Tables

List of Figures

Table S1. Observational data sets derived from satellite and ground-based measurements.

Quantity	Data set	Institution	Period	Grid res.	Step	Reference
Surface temperature (°C)	AMIP II v.1.1.3	PCMDI	1979–2010	1°	Monthly	Hurrell et al. (2008)
Near surface temperature (°C)	HadCRUT4 v.4.6.0	Met Office Hadley Centre, Climatic Research Unit, University of East Anglia	1988–2017	5°	Monthly	Morice et al. (2012)
Precipitation (mm day^{-1})	GPCP v.2.3	WCRP/GEWEX	1987–2016	2.5°	Monthly	Adler et al. (2003)
Mean sea level pressure (mb)	HadSLP2	Met Office Hadley Centre	1979–2004	5°	Monthly	Allan and Ansell (2006)
GPP (dg C m^{-2} $year^{-1}$)	MOD17A2 v.55	Numerical Terradynamic Simulation Group, University of Montana	2000–2015	1 km	Monthly	Zhao et al. (2005)

Table S2. Data obtained from ERA-Interim reanalysis (Dee et al., 2011). All data had a 2.5°×2.5° horizontal resolution and covered the time span 1987–2016.

Quantity	Parameter	Stream	Time	Step
At pressure levels 50–1000 hPa:				
Air temperature (K)	130	MODA	–	–
Zonal wind (m s^{-1})	131	MODA	–	–
Meridional wind (m s^{-1})	132	MODA	–	–
Radiation budget:				
Surface sensible heat flux (J m^{-2})	146	MNTH	00:00,12:00	12
Surface latent heat flux (J m^{-2})	147	MNTH	00:00,12:00	12
Surface solar radiation downwards (J m^{-2})	169	MNTH	00:00,12:00	12
Surface thermal radiation downwards (J m^{-2})	175	MNTH	00:00,12:00	12
Surface net solar radiation (J m^{-2})	176	MNTH	00:00,12:00	12
Surface net thermal radiation (J m^{-2})	177	MNTH	00:00,12:00	12
Top net solar radiation (J m^{-2})	178	MNTH	00:00,12:00	12
Top net thermal radiation (J m^{-2})	179	MNTH	00:00,12:00	12
Total incoming solar radiation (J m^{-2})	212	MNTH	00:00,12:00	12
Water budget:				
Evaporation (m)	182	OPER	00:00,12:00	12
Total precipitation (m)	228	OPER	00:00,12:00	12
Total column water vapour (mm)	137	MODA	–	–
For meridional stream function:				
Surface pressure (Pa)	134	MODA	–	–

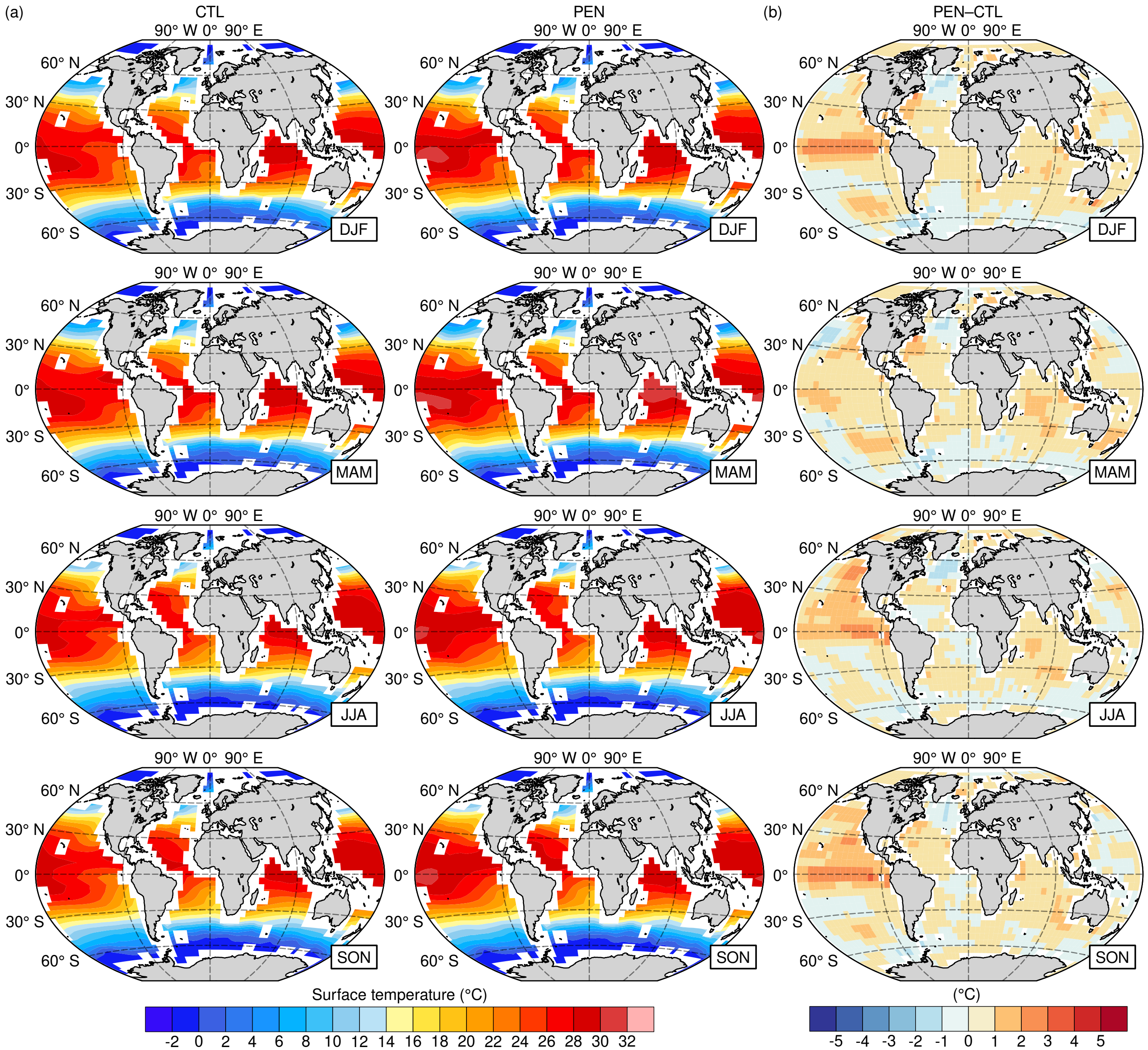

Figure S1. Prescribed SST climatology seasonal means for CTL and PEN simulations (a) and their absolute difference (b).

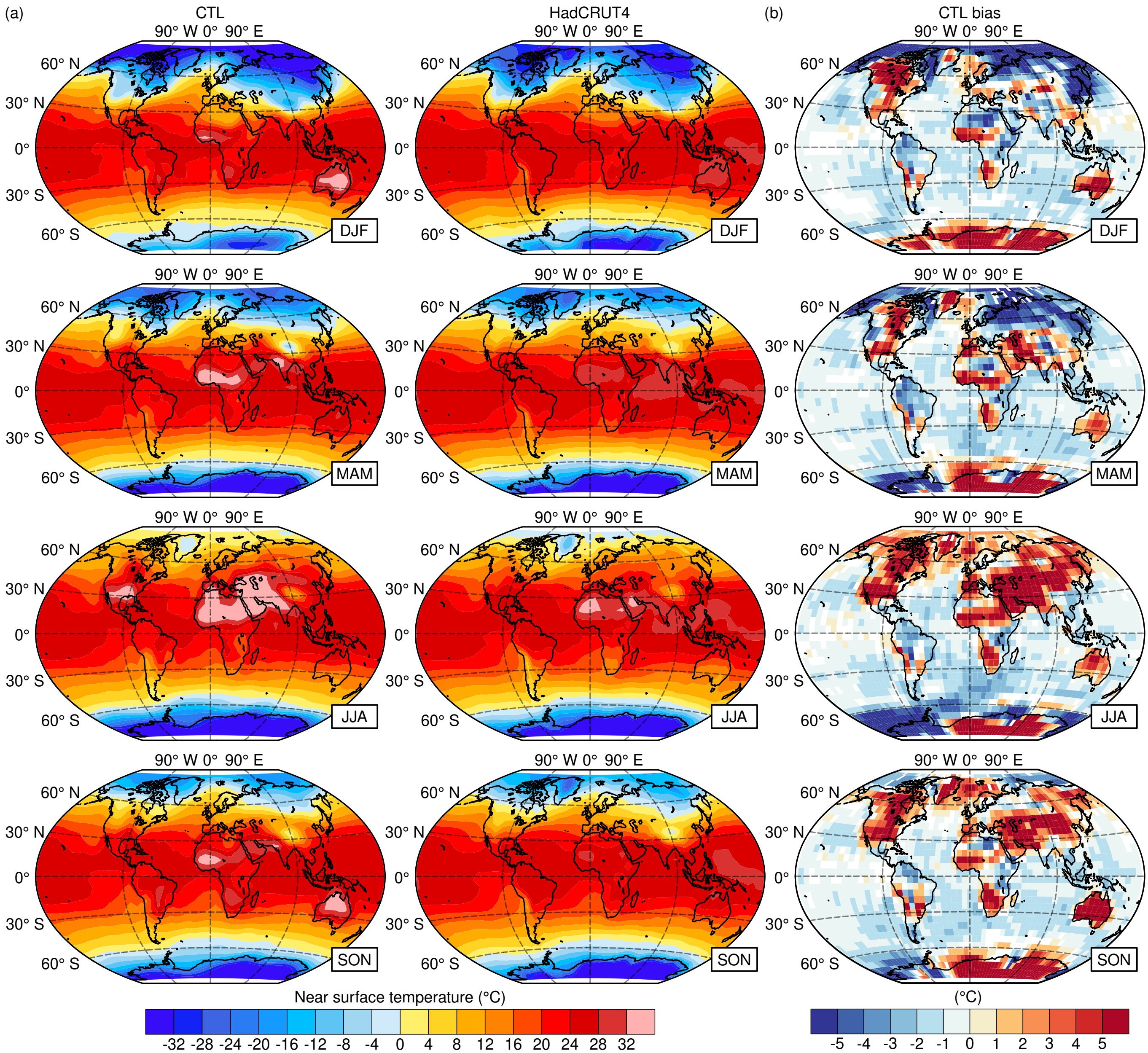

Figure S2. Seasonal means results of (a) near surface temperature for the CTL simulation and observational data from HadCRUT4 and (b) model bias. In the bias panels, white depicts gridpoints with statistically non-significant difference ($\alpha = 0.05$).

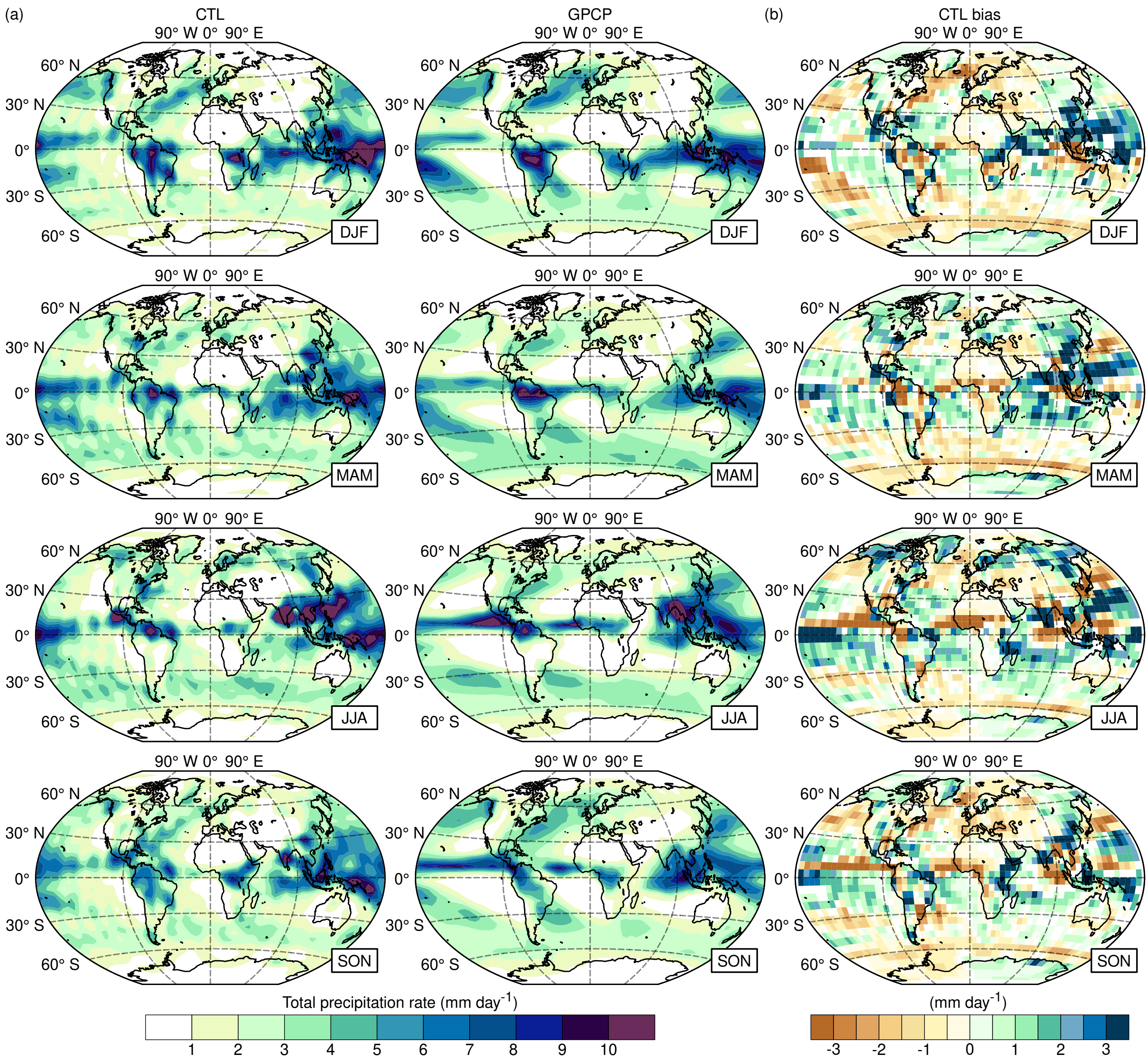

Figure S3. Seasonal means results of (a) total daily precipitation for the CTL simulation and observational data from GPCP and (b) model bias. In the bias panels, white depicts gridpoints with statistically non-significant difference ($\alpha = 0.05$).

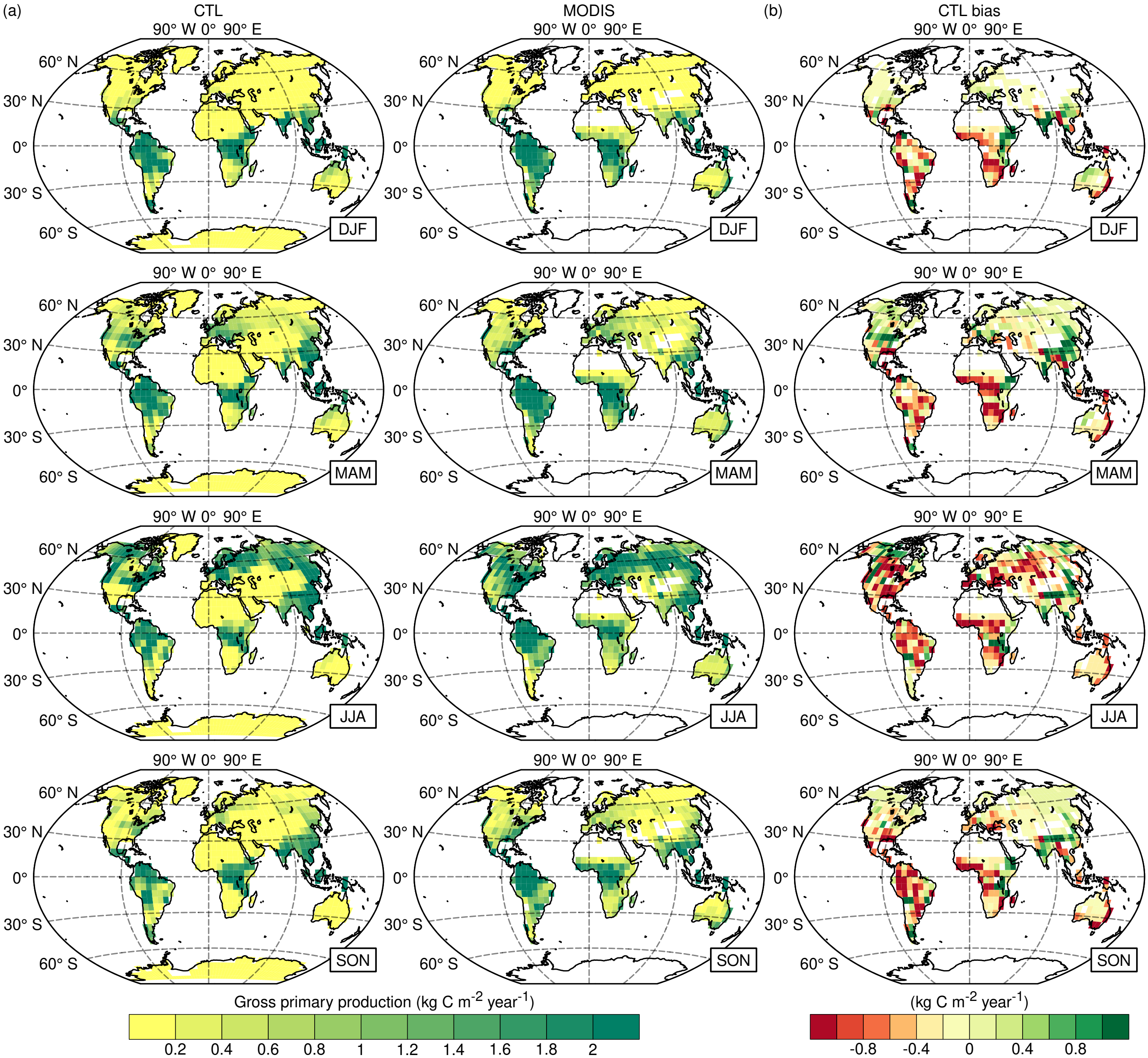

Figure S4. Seasonal means results of (a) GPP for the CTL simulation compared with observational data from MODIS and (b) model bias. In the bias panels, white is for statistically non-significant difference ($\alpha = 0.05$).

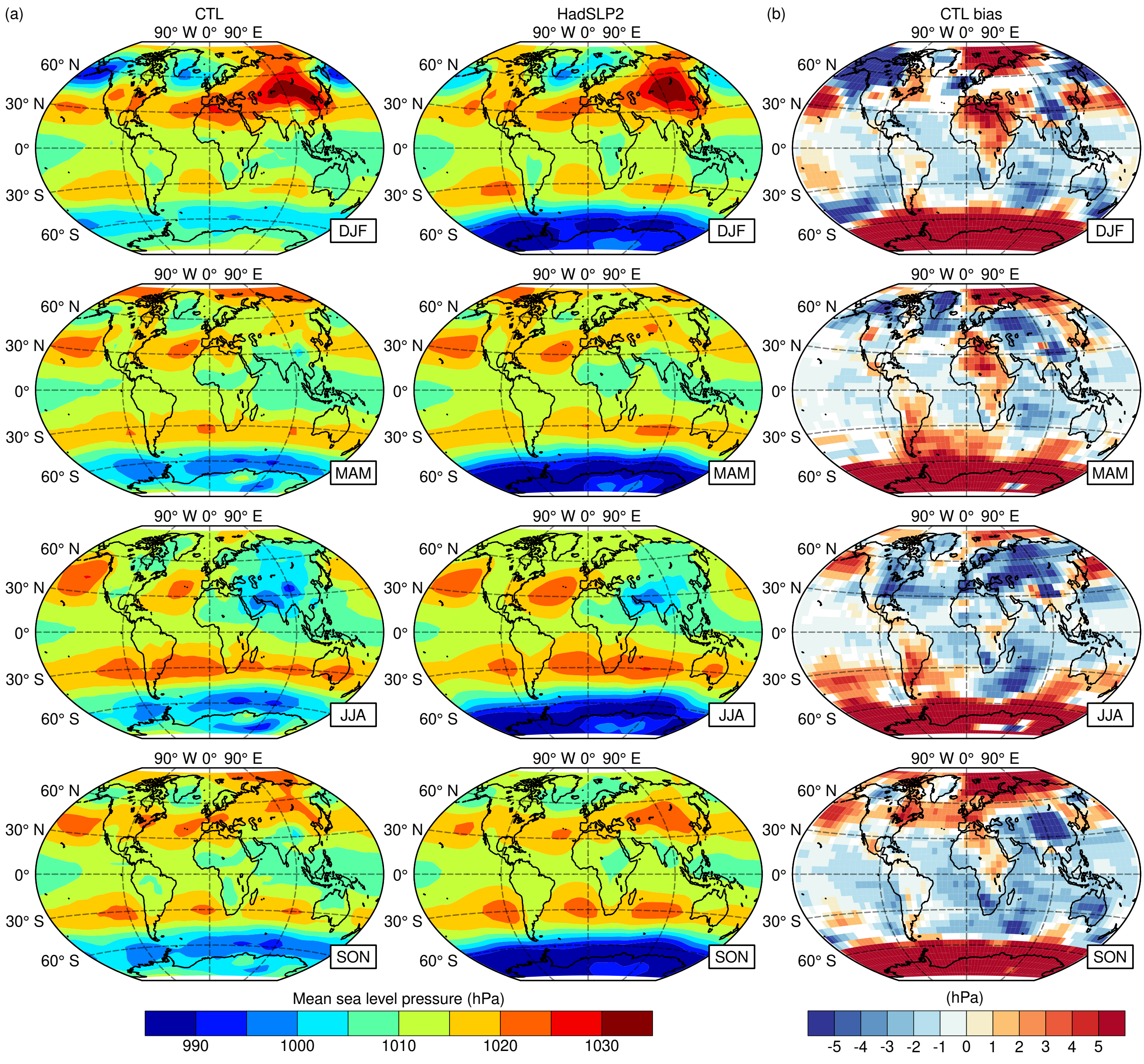

Figure S5. Seasonal mean results of (a) mean sea level pressure for the CTL simulation compared with observational data from HadSLP2 and (b) model bias. In the bias panels, white depicts gridpoints with statistically non-significant difference ($\alpha = 0.05$).

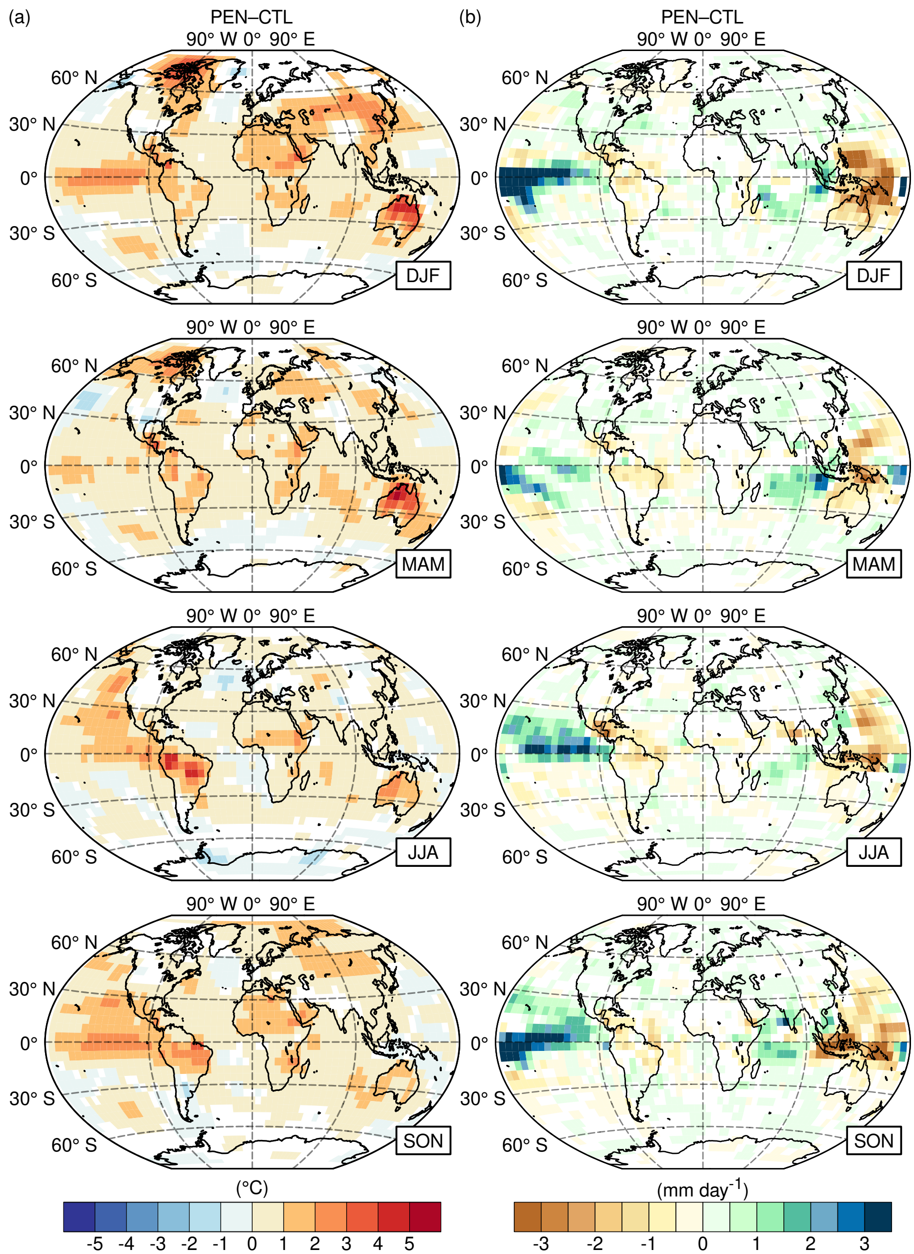

Figure S6. Differences in seasonal means results for the PEN simulation compared with the CTL simulation (PEN minus CTL) of (a) near surface temperature and (b) daily precipitation. In all panels, white depicts gridpoints with statistically non-significant difference ($\alpha = 0.05$).

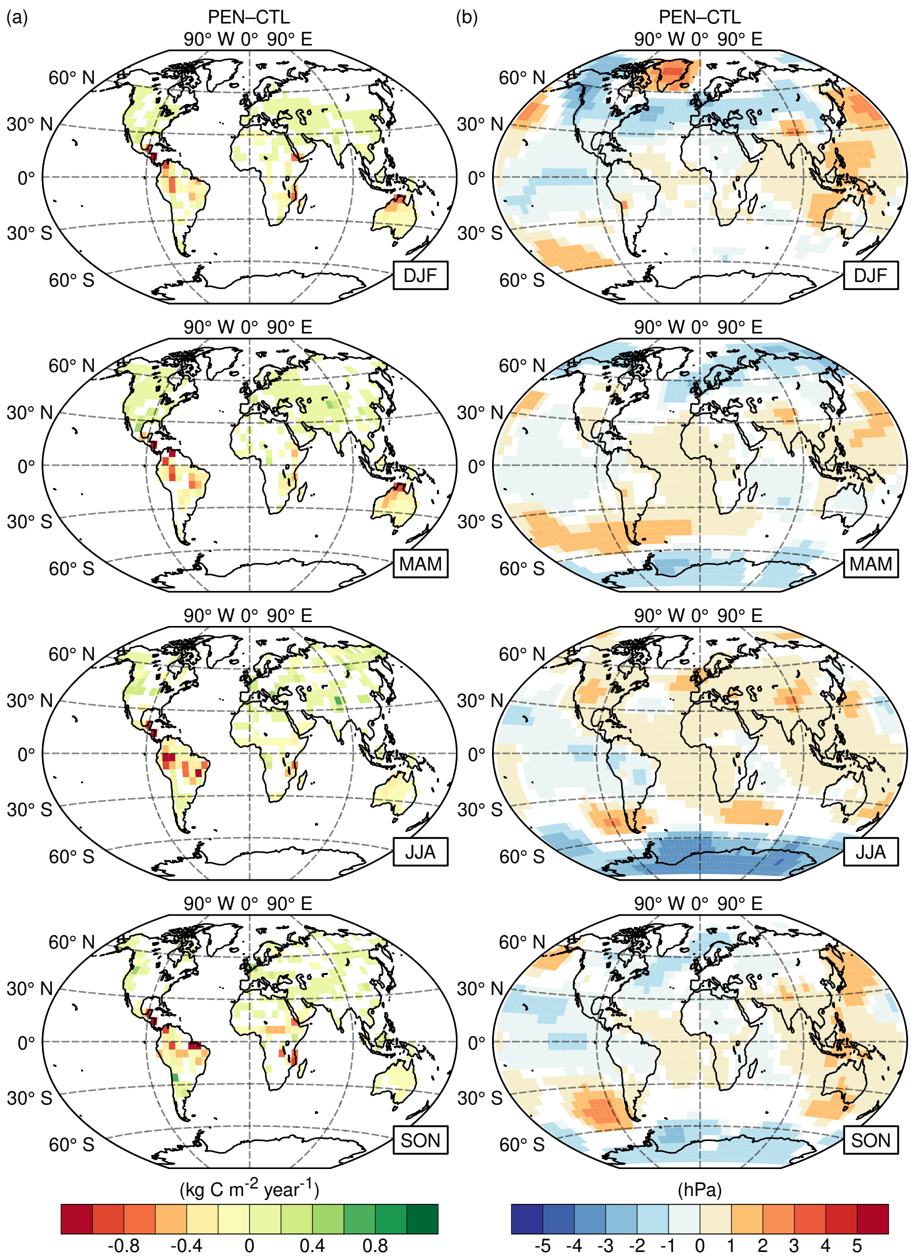

Figure S7. Differences in seasonal means results for the PEN simulation compared with the CTL simulation (PEN minus CTL) of (a) GPP and (b) mean sea level pressure. In all panels, white depicts gridpoints with statistically non-significant difference ($\alpha = 0.05$).

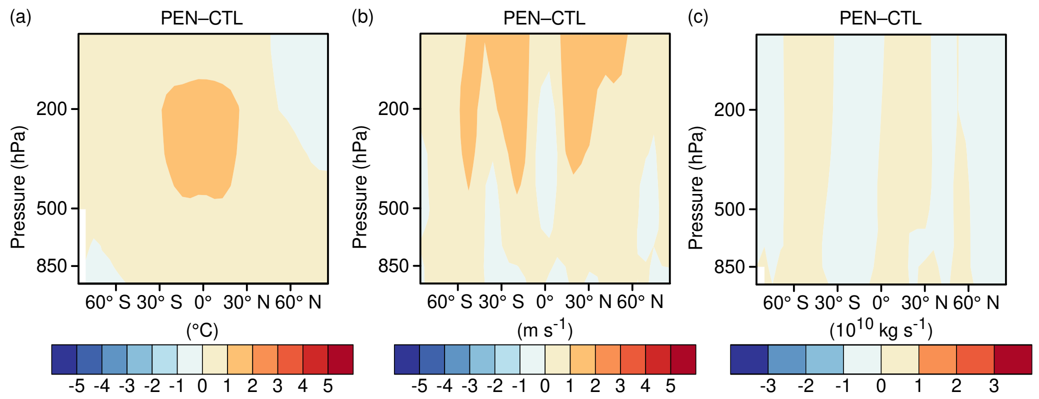

Figure S8. Differences in zonal average annual means for the PEN simulation compared with the CTL simulation (PEN minus CTL) at different pressure levels for: (a) air temperature, (b) zonal wind and (c) meridional stream function.

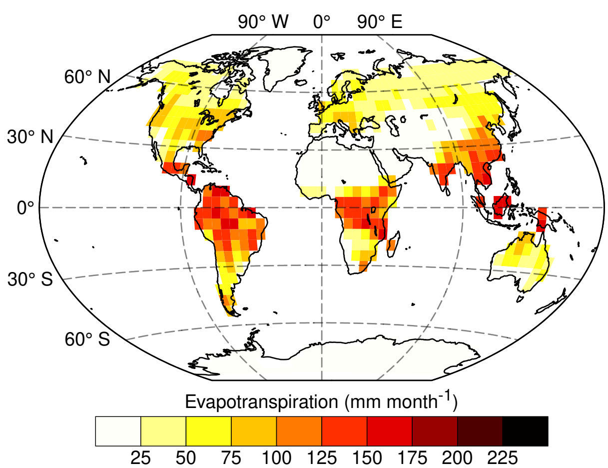

Figure S9. Annual mean evapotranspiration result for the CTL simulation used for the MCWD calculation.

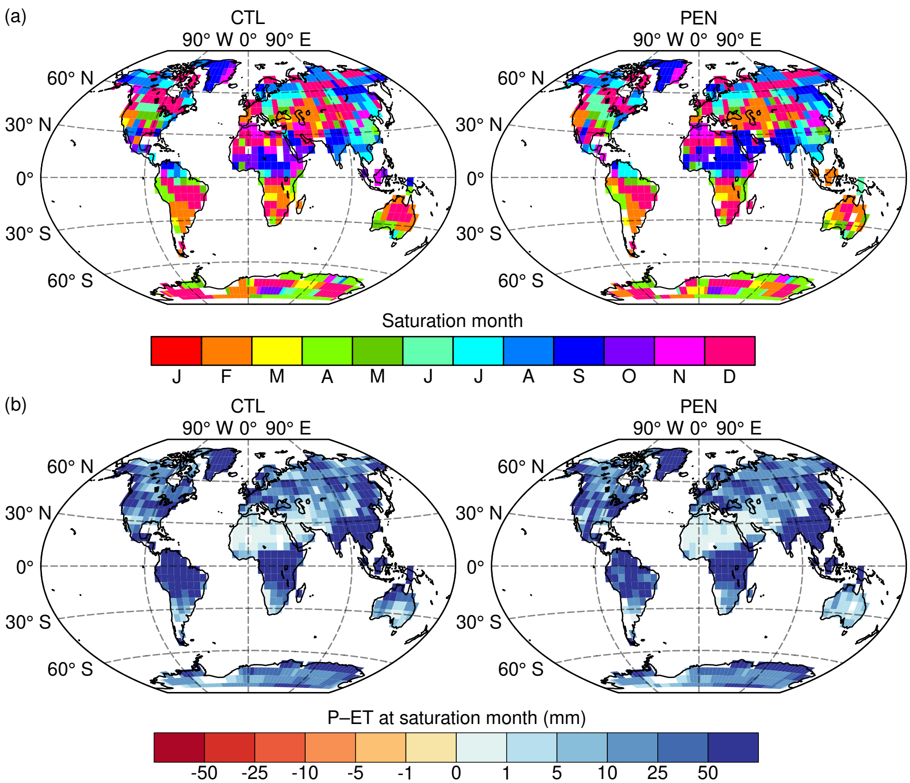

Figure S10. Saturation month (a) used in the calculation of MCWD. The first month is January and the last month is December. During these months precipitation (P) exceeded evapotranspiration (ET) in each gridpoint, saturating ground conditions (b). Water deficit accumulation is thus assumed to start at zero.

References

Adler, R. F., Huffman, G. J., Chang, A., Ferraro, R., Xie, P.-P., Janowiak, J., Rudolf, B., Schneider, U., Curtis, S., Bolvin, D., et al.: The Version-2 Global Precipitation Climatology Project (GPCP) Monthly Precipitation Analysis (1979-Present), Journal of Hydrometeorology, 4, 1147–1167, https://doi.org/10.1175/1525-7541(2003)004<1147:TVGPCP>2.0.CO;2, 2003.

Allan, R. and Ansell, T.: A New Globally Complete Monthly Historical Gridded Mean Sea Level Pressure Dataset (HadSLP2): 1850-2004, Journal of Climate, 19, 5816–5842, https://doi.org/10.1175/JCLI3937.1, 2006.

Dee, D. P., Uppala, S. M., Simmons, A. J., Berrisford, P., Poli, P., Kobayashi, S., Andrae, U., Balmaseda, M. A., Balsamo, G., Bauer, P., Bechtold, P., Beljaars, A. C. M., van de Berg, L., Bidlot, J., Bormann, N., Delsol, C., Dragani, R., Fuentes, M., Geer, A. J., Haimberger, L., Healy, S. B., Hersbach, H., Hólm, E. V., Isaksen, L., Kållberg, P., Köhler, M., Matricardi, M., McNally, A. P., Monge-Sanz, B. M., Morcrette, J.-J., Park, B.-K., Peubey, C., de Rosnay, P., Tavolato, C., Thépaut, J.-N., and Vitart, F.: The ERA-Interim Reanalysis: Configuration And Performance Of The Data Assimilation System, Quarterly Journal of the Royal Meteorological Society, 137, 553–597, https://doi.org/10.1002/qj.828, 2011.

Hurrell, J. W., Hack, J. J., Shea, D., Caron, J. M., and Rosinski, J.: A New Sea Surface Temperature And Sea Ice Boundary Dataset For The Community Atmosphere Model, Journal of Climate, 21, 5145–5153, https://doi.org/10.1175/2008JCLI2292.1, 2008.

Morice, C. P., Kennedy, J. J., Rayner, N. A., and Jones, P. D.: Quantifying Uncertainties In Global And Regional Temperature Change Using An Ensemble Of Observational Estimates: The HadCRUT4 Data Set, Journal of Geophysical Research: Atmospheres, 117, 1–22, https://doi.org/10.1029/2011jd017187, 2012.

Zhao, M., Heinsch, F. A., Nemani, R. R., and Running, S. W.: ImprovementS Of The MODIS Terrestrial Gross And Net Primary Production Global Data Set, Remote Sensing of Environment, 95, 164–176, https://doi.org/10.1016/j.rse.2004.12.011, 2005.